Journal of Electronic Imaging

JElectronicImaging.org

Estimating accurate optical flow in the presence of motion blur

Zhigang Tu
Ronald Poppe
Remco Veltkamp

SPIE. IS&T imaging.org

Estimating accurate optical flow in the presence of motion blur

Zhigang Tu,* Ronald Poppe, and Remco Veltkamp
Utrecht University, Department of Information and Computing Sciences, Princetonplein 5, Utrecht 3584CC, Netherlands

Abstract. Spatially varying motion blur in video results from the relative motion of a camera and the scene. How to estimate accurate optical flow in the presence of spatially varying motion blur has received little attention so far. We extend the classical warping-based variational optical flow method to deal with this issue. First, we modify the data term by matching the identified nonuniform motion blur between the input images according to a fast blur detection and deblurring technique. Importantly, a downsample-interpolation technique is proposed to improve the blur detection efficiency, which saves 75% or more running time. Second, we improve the edge-preserving regularization term at blurry motion boundaries to reduce boundary errors that are caused by blur. The proposed method is evaluated on both synthetic and real sequences, and yields improved overall performance compared to the state-of-the-art in handling motion blur. *© 2015 SPIE and IS&T* [DOI: 10.1117/1.JEI.24.5.053018]

Keywords: optical flow estimation; blur detection; deblurring; blur boundary preservation.
Paper 15419 received May 28, 2015; accepted for publication Aug. 25, 2015; published online Sep. 25, 2015.

1 Introduction

Estimating a dense optical flow field between two consecutive frames is one of the most fundamental problems in computer vision because optical flow is widely used in object detection, recognition, and tracking, as well as in image alignment, compression, denoising, and deblurring. Tu et al.[1] gave an introduction about the applications of optical flow. Horn and Schunck[2] proposed the variational method, where a regularization term is incorporated into a data term to compute optical flow. The basic data term assumes that the brightness of a moving pixel remains constant over time. This is called the brightness constancy assumption (BCA). By quantitatively evaluating various optical flow algorithms, Barron et al.[3] found that the variational methods yield dense flow fields but are sensitive to outliers, because the BCA-based quadratic data term of Horn and Schunck is not robust. Negahdaripour[4] proposed a new definition of optical flow to encourage investigation of problems in dynamic scene analysis. Weber and Malik[5] pointed out there are several causes for a violation of the BCA. Most of these concern out-of-plane rotations or are due to overlapping regions. Other potential sources of BCA violations are noise and motion blur,[6] where the motion blur is the result of a relative movement of the camera and scene that causes neighboring pixel values to become averaged. It is challenging for traditional optical flow algorithms to produce accurate results. Motion blur degrades the image quality. Not only image details are lost, but also image intensities show more variation, which leads to a multiple correspondences problem as Li et al.[7] described: a pixel in the current image corresponds to multiple pixels in the subsequent image.

Motion blur is a common issue in videos, but it has not received much attention from the research community. One pioneering work is by Rekleitis,[8] who proposed a method to estimate optical flow from a single motion-blurred image using the information present in the structure imposed on the image by the motion blur. The information of the motion blur in the frequency domain is applied to extract the orientation and the magnitude of the displacement vector—the flow vector. In this work, we aim to treat this problem by extending the warping-based blur-robust flow baseline method of Portz et al.[9] with two modifications that explicitly address the motion blur in estimating optical flow from image sequences.

This paper is organized as follows. In the next section, we discuss the relation between optical flow and motion blur, and discuss methods that target this setting. We introduce the baseline optical flow algorithm in Sec. 3. Two extensions of the traditional optical flow formulation are described in Sec. 4. We experimentally validate our proposed methods in Sec. 5. A brief conclusion is given in Sec. 6.

2 Related Work on Optical Flow and Motion Blur

Motion blur often leads to a significant deterioration to the image. Especially in low-light conditions, where less light is available and longer exposure times are needed, the captured image often ends up blurry. Additionally, more noise is introduced. Recovering the latent image from a single blurred image is known as an inherently hard ill-posed problem. Typically, two steps are implemented to deblur an image. First, with blind deconvolution, the blurred image is modeled as a latent image convolved with a blur kernel, and the underlying blur kernel is obtained by deconvolution. Second, using nonblind deconvolution, the deblurred image is further refined by solving a nonblind deconvolution problem with the estimated kernel.

Single image blind deconvolution techniques have been largely advanced recently, and perform well on noise-free images. For example, Xu and Jia[10] found that strong edges are not always beneficial for kernel estimation and can degrade it under certain conditions. They presented a new method to measure the usefulness of image edges in motion deblurring and a gradient selection approach to

*Address all correspondence to: Zhigang Tu, E-mail: Z.Tu@uu.nl

mitigate their possible adverse effects. Goldstein and Fattal[11] proposed to recover the blur kernel in motion-blurred images according to the statistical deviations they exhibit in their spectrum. This method can identify a set of statistics, and after appropriately whitening its spectrum, this information is used to recover the blur. The blur kernel is estimated by employing a phase retrieval algorithm with improved convergence and disambiguation capabilities. However, they are sensitive to image noise since even a small amount of noise can degrade the quality of blur kernel estimation. Yitzhaky and Kopeika[12] identified important blur parameters from filtered motion blurred images with which to characterize the point spread function of the blur. If the identification can be correctly carried out, the image can be deblurred quickly with high resolution. A breakthrough work in image deblurring is the work of Cho and Lee,[13] where both latent image estimation and kernel estimation are efficiently carried out in an iterative deblurring process by introducing a novel prediction step under a coarse-to-fine framework. Importantly, they use image filters to suppress noise at their prediction step. However, due to the side effects of denoising, a biased blur kernel is obtained. Sun et al.[14] applied the observed image gradients to compute the parameters of motion blur (i.e., orientation and extension). One advantage of this method is that the proposed normalized Radon transform from the blurred image gradients can be used to estimate the motion blur parameters from noisy image gradients. Tai and Lin[15] applied an existing denoising package of Neat image team–NeatImage[16] to preprocess the input image. Then they iteratively employed a motion-aware nonlocal mean filter and a deblurring process to refine the results. Since both the denoising package and the nonlocal means filter have the same negative impacts on the kernel calculation, the estimated kernel is still not accurate.

Recently, Zhong et al.[17] handled these problems by applying a directional low-pass filter to the input image. The directional filter reduces the noise level, while the frequency content including essential blur information along the orthogonal direction is preserved. Their improved framework produces better kernels with a low run-time. Derived from Zhong et al.,[17] Li et al.[7] proposed a directional high-pass filter to refine the pre-estimated blur kernel which is computed by the fast blind deconvolution method of Cho and Lee.[13] In this work, we employ the directional filter technique to refine the estimated blur kernel, which is effective for improving the deblurring performance and the accuracy of the estimated flow field.

More importantly, instead of using the full blurry image for deblurring, we adopt the strategy of Shi et al.[18] The first step is to detect blurred pixels and segment the image into blurred and clean regions. Then deblur only those pixels inside blur masks using the procedure described in Xu and Jia.[10] Finally, put the original clean region back in the deblurred image. Hu and Yang[19] stated that not all pixels of the input blurry image are informative. In other words, if the whole image is used for deblurring, this is likely to result in degraded results. Consequently, it is preferable to detect and use effective blur features rather than the whole image for deblurring. Shi et al.[18] presented a blur detection maps technique to extract blur regions by constructing blur feature representations. This method can effectively detect blur pixels but is computationally expensive. To improve the efficiency, we present a downsampling-interpolation technique which can significantly reduce the computation time.

The homogeneous regularization term in the Horn and Schunck[2] model does not respect flow discontinuities, and brings out over-smoothing at motion boundaries. Alvarez et al.[20] proposed an isotropic image-driven regularizer to suppress smoothing at image boundaries, while an anisotropic regularizer was introduced by Alvarez et al.[21] to suppress smoothing across the image boundaries. Schnorr[22] designed an isotropic flow-driven regularizer to reduce smoothing at motion boundaries while avoiding over-segmentation of strong textured structures. Weickert and Schnorr[23] constructed an improved anisotropic flow-driven regularizer, which achieved smoother effects along flow discontinuities while at the same time producing fewer fluctuations.

At present, the advanced motion and structure-adaptive regularization term is widely used for preserving edges (i.e., Wedel et al.[24] and Xu et al.[25]), and it favors motion discontinuities to coincide with discontinuities of the image structures. Normally, motion discontinuities arise at object boundaries where the BCA is likely to change. If the input image contains motion blur, the BCA is violated. The pixel values are combined from multiple surfaces, especially at motion boundaries. Even worse, the changes of the brightness of the edge pixels no longer correspond to the changes of the motion at boundaries. Hence, the brightness gradient-based weight is not valid at the blurry boundaries. To overcome this problem, in this work, we first extract the blurry boundaries with the fast Canny detector, and then reset the weights at these positions. With this contribution, motion errors at blurry boundaries are reduced while edges are well-preserved.

Our work is related to the methods of Portz et al.[9] and Li et al.[7] The blur-robust flow energy formulation and the directional high-pass filter are used to compute optical flow in terms of interleaving an iterative blind deconvolution and a warping-based minimization. In particular, we make three improvements to Portz et al.[9]

- Instead of deblurring the whole image, we segment the image into blur and clean regions with the discriminative blur maps technique, and solely deblur the extracted blurry regions.
- To improve the efficiency, we propose a downsample-interpolation technique during the blur detection. As the flow is computed in a coarse-to-fine manner, we select the downsampled second level image for blur detection. Then we upsample the labeled image (i.e., detected blur features are set to 1 and clean regions pixels are set to 0) to the initial size by bilinear interpolation. Since the coarser levels images contain reduced amounts of blur, we only implement the local deblurring on the first level (i.e., the initial image size).
- To better preserve edges of the estimated flow field, we use the edge-preserving regularization method. We extend this method by detecting the blurry edges of the input image and assign more accurate weights to them to reduce biases at the blurry motion boundaries.

3 Blur-Robust Optical Flow Algorithm

If one or both of the input images contain motion blur, the BCA-based data term will be violated. Moreover, because

minimizing the classical warping-based optical flow method depends on warping the source image to match the appearance of the target image under the constraint of the data term, unpredictable flow errors will be produced across different motion blur regions. To handle this problem, Portz et al.[9] presented an improved brightness constancy data term to obtain a more accurate flow by matching the nonuniform motion blur between the image pair. We discuss the original warping-based optical method of Horn and Schunck[2] and the improved version of Portz et al.[9] subsequently.

3.1 *Baseline Warping-Based Optical Flow Method*

Optical flow refers to the apparent motion pattern between input frames I_1 and I_2, and describes how corresponding pixels in consecutive frames match. Normally, it is computed by minimizing an energy function which is formulated as a weighted sum of a data term and a regularization term

$$E(u,v) = E_D(u,v) + \lambda E_S(u,v), \tag{1}$$

where $\mathbf{w} = (u,v)$ is the flow field, and the direction and magnitude of its each flow component indicates where and how a pixel moved between I_1 and I_2.

$E_D(u,v)$ is the data term, which assumes the brightness of a pixel remains the same under its displacement

$$E_D(u,v) = \int_\Omega \Psi_D(\{I_2[\mathbf{x}+\mathbf{w}(\mathbf{x})] - I_1(\mathbf{x})\}^2)\mathrm{d}x\mathrm{d}y, \tag{2}$$

where Ψ_D is a penalty function, and $\mathbf{x} = (x,y)$ denotes a point in the image domain Ω. As Sun et al.[26] stated: the less-robust Charbonnier is preferable to the highly nonconvex Lorentzian and a slightly nonconvex penalty function ($\alpha = 0.45$) is better still, therefore, we select the generalized Charbonnier penalty function of Sun et al. for our model, where $\Psi_D = \Psi(s^2) = (s^2+\xi^2)^\alpha$, $\xi = 0.001$, and $\alpha = 0.45$.

$E_S(u,v)$ is the regularization term, which quantifies the smoothness of the flow field

$$E_S(u,v) = \int_\Omega \Psi_S(|\nabla u|^2 + |\nabla v|^2)\mathrm{d}x\mathrm{d}y, \tag{3}$$

where Ψ_S is same as Ψ_D. The robust regularization term is used to solve the aperture problem and also allows us to deal with outliers. λ is the regularization parameter, which determines the balance between the data term and the regularization term (Tu et al.[27]).

3.2 *Blur-Robust Optical Flow Method*

A natural motion blurred image I can be generally modeled as

$$I = k * L + n, \tag{4}$$

where k represents a motion blur kernel, L is the latent image of I, n represents the unknown noise introduced during image acquisition, and *; denotes the convolution operation. Both k and L can be efficiently estimated from I by the fast blind deconvolution deblurring method of Cho and Lee.[13]

In optical flow estimation, the observed input images I_1 and I_2 can be expressed as $I_1 = k_1 * L_1$ and $I_2 = k_2 * L_2$, where k_1 and k_2 are spatially varying or spatially invarying blur kernels. To address the motion blur issue, Portz et al.[9] and Li et al.[7] modify the data term by matching the nonuniform motion blur between I_1 and I_2. The estimated blur kernels k_1 and k_2 are applied to the other, respectively, to construct a newly motion blur uniform image pair (B_1, B_2)

$$B_1 = k_2 * I_1 \approx k_2 * k_1 * L_1, \tag{5}$$

$$B_2 = k_1 * I_2 \approx k_1 * k_2 * L_2. \tag{6}$$

To better preserve edges, the advanced edge-preserving regularization term is applied, which is defined as

$$E_S(u,v) = \int_\Omega \omega(\mathbf{x})\Psi_S(|\nabla u|^2 + |\nabla v|^2)\mathrm{d}x\mathrm{d}y. \tag{7}$$

$\omega(\mathbf{x})$ is a simple structure-adaptive map that maintains motion discontinuity:

$$\omega(\mathbf{x}) = \exp(-\|\nabla I_C\|^\gamma), \tag{8}$$

where I_C is the color vector in the CIELab space of I_1, and we set $\gamma = 0.8$ according to Xu et al.[25]

The improved edge-preserving blur-robust optical flow energy function can be expressed as

$$E(u,v) = \int_\Omega \Psi_D(\{B_2[\mathbf{x}+\mathbf{w}(\mathbf{x})] - B_1(\mathbf{x})\}^2)\mathrm{d}x\mathrm{d}y + \lambda \int_\Omega \omega(\mathbf{x})\Psi_S(|\nabla u|^2 + |\nabla v|^2)\mathrm{d}x\mathrm{d}y. \tag{9}$$

The well-known numeric optimization method of Brox et al.[28] which implements a two nested fixed point iteration scheme in the coarse-to-fine framework, is used for computing the optical flow.

A directional filter is effective to reduce noise while preserving the blur information in the orthogonal direction to the filter. Li et al.[7] designed a directional high-pass filter to refine the pre-estimated blur kernels k_1 and k_2 before minimizing the blur-robust optical flow energy function. We introduce the directional filter technique in this work to improve the deblurring performance to obtain a more accurate flow field.

4 Improved Edge-Preserving Blur-Robust Optical Flow Algorithm

The state-of-the-art optical flow method of Portz et al.[9] based on the classical coarse-to-fine warping manner has achieved accurate flow in the presence of spatially varying motion blur, but it still has two severe drawbacks. In this section, two effective approaches are described to handle these two problems, respectively.

4.1 *Downsample Interpolation–Based Efficient Learned Blur Maps Method*

Commonly, the input images I_1 and I_2 contain motion blur, but not all pixels are useful for deblurring. In addition, some useful information belonging to clean regions' pixels is removed due to the complete deblurring. To avoid these side effects, segmenting the image into blurred and clean parts and deblurring only the identified blur regions should

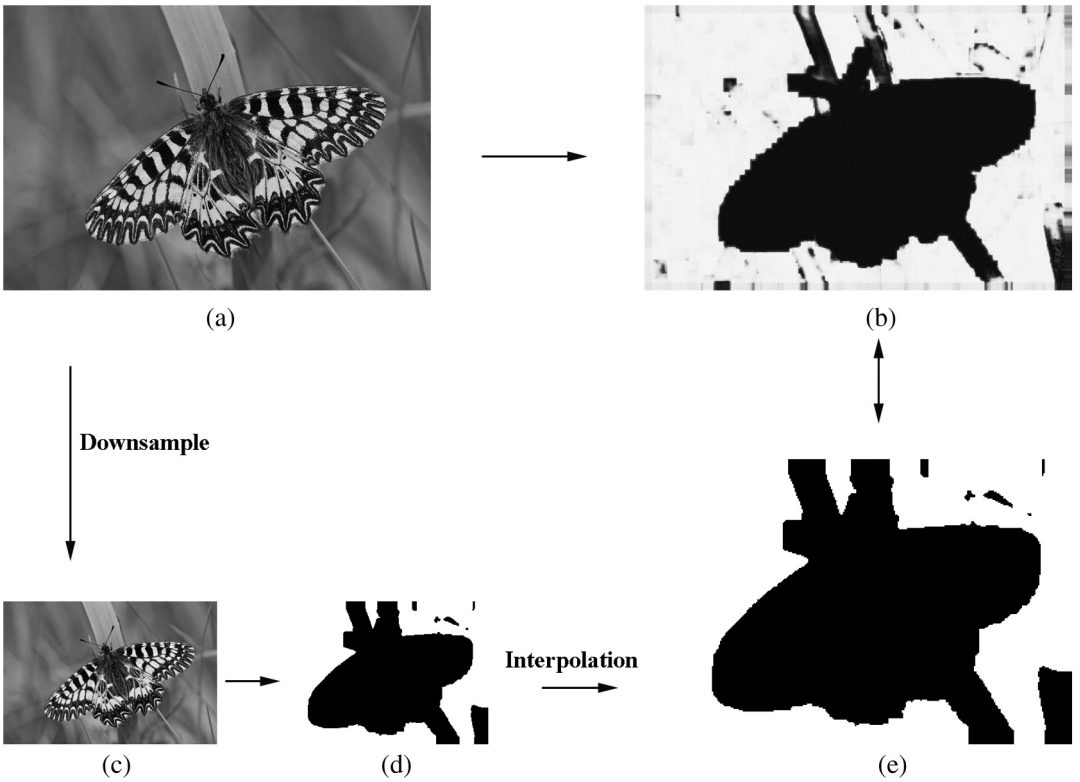

Fig. 1 Demonstration of the downsample–interpolation based blur detection technique: (a) input initial image I_1, (b) blur detection with method Shi et al.[18] on I_1, (c) downsampled image I_{1L2}, (d) blur detection on I_{1L2}, and (e) interpolation.

yield better results. How to effectively and efficiently detect blur pixels is an important task.

Shi et al.[18] addressed this problem by finding and constructing a few local blur feature representations that consider image gradient, Fourier domain descriptor, and data-driven local filters. Each of the blur feature representations is potent enough to differentiate between the clean and blurred regions. More importantly, these features perform independently but are complementary to each other. To combine these features, a naive Bayesian classifier is used to naturally integrate them in a discriminative way and to form a blur maps method.

The blur maps method can accurately detect blur pixels, but it is not efficient. The computational cost is exponentially increased, especially for high-resolution images. In particular, when using it in the optical flow estimation, the blur detection process costs more than 80% of the total run time. To improve the efficiency of Shi et al.,[18] we introduce a downsample-interpolation approach. As shown in Fig. 1, we use the down-sampled butterfly images I_{1L2} and I_{2L2} ($L2$ denotes the second pyramid level) for blur detection. Since the downsampled image, e.g., I_{1L2}, is much smaller than the initial input image I_1, the computation time of the blur detection is significantly decreased. After that, we interpolate the downsampled labeled binary image to the initial size by using the bilinear method. Table 1 reveals that our downsample interpolation–based blur detection approach is approximately 15 times faster than the baseline method. The blur detection is a little bit different between our downsample-interpolation method and that of Shi et al.,[18] but the accuracy of the flow estimation is not affected because the miss detected blurred pixels in the coarse scale are labeled again after the interpolation process in the original resolution. Furthermore, Cho and Le[13] stated that motion blur was reduced in coarser levels of the downsampled pyramid in the coarse-to-fine framework. This is because the extent of blur is narrowed in coarser scale images. According to this statement, we only perform blur detection and deblurring for the original input images and do not implement this operation for its down-sampled variations in the coarser levels during optical flow estimation. By taking this implementation, the computational time is further saved while the flow accuracy is not affected as the flow is refined in the original input images.

4.2 *Improved Edge-Preserving Regularization*

The regularization term, which is the basic component of variational optical flow algorithms, quantifies the smoothness of the flow field and prefers motion discontinuities coincide with brightness discontinuities. Constructing an image structure-adaptive regularization term is suitable to preserve flow edges and to improve the performance of optical flow estimation. However, for the motion blur image, especially at motion boundaries, the brightness derivative weights of the regularization term [Eq. (7)] are violated. Since each of the pixel values at blur boundaries is a combination of information from multiple surfaces, the gradient cannot correctly reflect the correspondence between the pixel brightness change and its motion change. In other words, the blurred boundary pixel is not the truth of itself, and this results in its gradient based weight not being accurate. On the other hand, for nonboundary blurred pixels, due

Table 1 Execution time of the blur detection on butterfly sequence for the blur maps method of Shi et al.[18] and our downsample-interpolation technique (both are reported on CPU).

	Blur maps	Downsample-interpolation
Time(s)	1658.4	113.8

to the uniform distribution of the brightness, their derivatives are very small which means that their gradient weights are close to 1. Consequently, we only need to label the blurry boundary pixels L_B and reset their gradient weights to 1. Based on this characteristic, an improved edge-preserving regularization (IEPR) term can be formed, and the modified structure-adaptive map is defined as

$$\omega'(\mathbf{x}) = L_B + (1 - L_B) \cdot \exp[-\left\|(1-\beta)\nabla I_C + \beta \nabla I_2(\mathbf{x}+\mathbf{w})\right\|^{\gamma}], \quad (10)$$

where L_B is the label of the detected blur boundary pixels. I_C is the color vector in the CIELab space. γ is same as in Eq. (8). $\beta = 0.05$ is used to construct a blended version of the derivative. The classical structure-adaptive map favors discontinuities of the motion field to arise at locations of strong image gradient. However, the intermediate motion field relies on both the reference image I_1 and the warped interpolation image $I_2(\mathbf{x}+\mathbf{w})$, which means that, in theory, our blended method should outperform those of Wedel et al.[24] and Xu et al.[25] A similar approach has been proposed in Wedel et al.[29] As both images contribute to the gradient, larger flow vectors can be matched and better results are obtained. Figure 2 shows the process to improve the edge-preserving regularization by weighting the detected blur boundary pixels and nonboundary pixels, respectively. The improvement from the blended derivative is demonstrated in Table 2.

Table 2 Average endpoint error (AEE) for the spatially varying motion blur sequences *ambush2* and *market5* from MPI Sintel benchmark with four different implementations.

Final pass	ambush2	market5
FD + EPR	37.373	21.313
FD + IEPR (No blend)	37.236	21.288
FD + IEPR	37.145	21.195
DD + IEPR (ours)	36.690	20.565

5 Experiments

We evaluate the accuracy of our optical flow algorithm on both synthetic and real sequences with spatially varying motion blur. In particular, quantitative and visual comparisons are conducted between the proposed algorithm and three existing state-of-the-art optical flow methods: Brox et al.,[28] Xu et al.,[25] and Portz et al.[9] The method of Brox et al.[28] is the basis of many popular variational optical flow algorithms, and its optimization framework and numerical scheme are employed in our method. The motion detail preserving (MDP) method of Xu et al.[25] is one of the best performing optical flow methods without considering the motion blur. Recently, Portz et al.[9] extended the classical warping-based optical flow method of Brox et al.[28] to achieve accurate flow in the presence of spatially varying motion blur, which represents the state-of-the-art technique that can handle motion blur in the flow estimation. Importantly, the three implementations are publicly available. In all cases, we used the original parameters. The experiments are performed on a laptop with an Intel Core i5-2410M 2.30 GHz processor and 4-GB memory.

To quantitatively evaluate the motion estimation accuracy, we use two kinds of error measures for comparison. First,

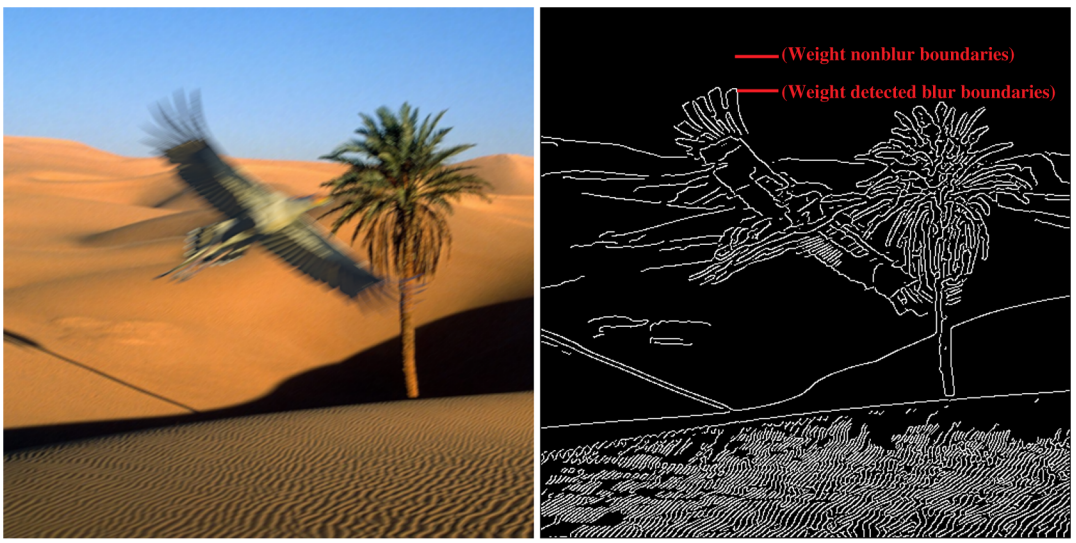

Fig. 2 Improving the edge-preserving regularization: (a) frame 5 of the *desert* sequence and (b) detecting blur boundary pixels and labelling them as L_B, then weighting the labeled pixels L_B with 1, and weighting the nonboundary pixels in terms of the blended version of the derivative.

the common average endpoint error (AEE) of Baker et al.[30] is applied to compare the computed dense flow fields of each method. Second, in the presence of motion blur, the intensity value of the original image is violated, which results in a multiple-correspondence problem: a point in I_1 corresponds to multiple points in I_2. To reduce the effect of this, we introduce the sampled average endpoint error (SAEE) of Li et al.[7] for evaluation, which is defined as

$$\text{SAEE} = \text{mean}[\sqrt{(\bar{u}_\text{T} - \bar{u})^2 + (\bar{v}_\text{T} - \bar{v})^2}], \tag{11}$$

where $\bar{\mathbf{w}}_\text{T} = (\bar{u}_\text{T}, \bar{v}_\text{T})$ is the sampled ground truth and $\bar{\mathbf{w}} = (\bar{u}, \bar{v})$ is the sampled estimated flow. The sample process is executed according to

$$|I_2(\mathbf{x} + \bar{\mathbf{w}}) - I_1(\mathbf{x})| < \varepsilon, \tag{12}$$

where $\bar{\mathbf{w}} \subset \mathbf{w}$, ε is a threshold.

5.1 *Synthetic Sequence Evaluation*

Sequences *ambush2* and *market5* from the final pass of the challenging MPI Sintel benchmark of Butler et al.[31] are selected to evaluate the effectiveness of our discriminative blur detection and deblurring technique as well as the IEPR. These two sequences contain severe spatially varying motion blur and defocus blur. Table 2 shows the average AEE of all frames of each sequence under four different implementations: (1) fully deblurring (FD) together with the general edge-preserving regularization (FD + EPR), (2) fully deblurring together with the proposed IEPR under two additional conditions: without blend derivative [FD + IEPR (NoBlend)], (3) with blend derivative (FD + IEPR) and, (4) our advanced method—discriminative blur detection and deblurring together with the IEPR (DD + IEPR). Table 2 shows that the flow accuracy is improved with our DD technique and our IEPR technique. More importantly, combing these two techniques further modifies the flow accuracy in the presence of motion blur.

Next, we choose two kinds of typical motion blur synthetic sequences to test the overall performance of our improved edge-preserving blur-robust flow method.

5.1.1 *Sequence with static background*

In this experiment, the *Astronaut* sequence, which is generated by varying the exposure time between frames and moving the foreground objects, is used for comparison. The *Astronaut* not only contains heavy noise, but different frames have different motion blur. Figure 3 shows the estimated flow fields of the four methods from a blurry frame to a relatively sharp frame. It is clear that the typical warping-based methods of Brox et al.[28] and Xu et al.[25] without nonuniform motion blur processing fail to recover the motion. Especially for Brox et al.[28] [see Fig. 4(a)], the flow is too blurred to identify any object. The state-of-the-art baseline method Portz et al.[9] is also not accurate. For example, the motion boundaries are distorted. In contrast, our estimated flow [Fig. 3(d)] is much more accurate. The motion boundaries are better preserved, and the legs of the astronaut which cannot be discerned in Portz et al.,[9] are well recovered. Furthermore, noise is effectively removed.

5.1.2 *Sequence with moving foreground and background*

In the third experiment, shown in Figs. 4 and 5, we choose the sequences *elephant* and *desert* for testing from Wul and Black.[32] For each sequence, all frames have significant motion blur, and both the foreground and background are moving. It is easy to find that without debluring, the flow

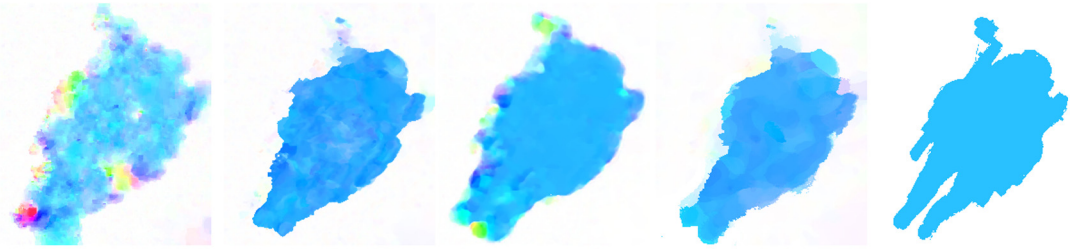

(a) (b) (c) (d) (e)

Fig. 3 Visual comparison on the synthetic sequence *astronaut*. Results of: (a) Brox et al.,[28] (b) Xu et al.,[25] (c) Portz et al.,[9] (d) ours, and (e) ground truth.

(a) (b) (c) (d) (e)

Fig. 4 Visual comparison on the synthetic sequence *elephant*. Results of: (a) Brox et al.,[28] (b) Xu et al.,[25] (c) Portz et al.,[9] (d) ours, and (e) ground truth.

(a) (b) (c) (d) (e)

Fig. 5 Visual comparison on the synthetic sequence *desert*. Results of: (a) Brox et al.,[28] (b) Xu et al.,[25] (c) Portz et al.,[9] (d) ours, and (e) ground truth.

results of Brox et al.[28] contain a large number of errors. The estimation accuracy of the MDP method is much better than that of Brox et al.[28] However, due to the lack of deblurring, the biases caused by the blur are distributed around its flow field [see Fig. 4(b)]. Additionally, some structures are inaccurately recovered. In Fig. 5(b), the estimated wing is inconsistent with the real object. Moreover, the spindly plumage is imprecisely captured and the head is lost. Surprisingly, the state-of-the-art optical flow algorithm of Portz et al.,[9] which includes the spatially varying motion blur handling mechanism, fails to estimate the motion of the foreground eagle. In particular, the motion boundaries are too blurry and the recovered shapes are far from the ground truth. Our method outperforms all other algorithms. The flow shapes are correctly recovered and the motion boundaries are sharp enough to distinguish the moving object [see Figs. 4(d) and 5(d)]. However, one problem of our method is that the deblurring process also removes some useful detailed information, leading to some small structures that are not well estimated. Table 3 shows the quantitative comparison in terms of AEE and SAEE, which demonstrates that our method yields significant improvements over the other techniques. In particular, comparing to the state-of-the-art baseline method of Portz et al.,[9] the accuracy of our method is more than 10% enhanced. In addition, our method is much more efficient than Portz et al.,[9] generally, four or more times faster. The higher the resolution of the input frames, the faster our method is than that of Portz et al.[9]

5.2 *Real Sequence Evaluation*

Two kinds of real sequences are used to evaluate the ability of our method.

5.2.1 *Sequence with static background*

In this experiment, we use the sequences *magazine* and *hand* for evaluation. The backgrounds in these sequences are static. The flow results of Portz et al.[9] and Brox et al.[28] contain many errors. For example, the motion blur causes biases [see Figs. 6(b), 6(d), 7(b), 7(d)]. Not only can some motion blur pixels not be correctly matched, but also some non-blurred pixels are mismatched. The MDP method produces a more accurate flow than the methods of Portz et al.[9] and Brox et al.[28] However, it fails at motion boundaries and some blurry texture-less regions. In contrast, as shown in Figs. 6(e) and 7(e), due to our segmented deblurring technique and the IEPR, motion boundaries are precisely recovered. Moreover, biases caused by the motion blur in the detected blur regions are greatly reduced. In addition, since we do not implement deblurring at clean regions, some useful information is well-preserved and precise motion estimation is obtained.

5.2.2 *Sequence with moving foreground and background*

Two real sequences *sign* and *bike*, with both foreground objects and background moving, are selected for testing. As shown in Figs. 8 and 9, flow fields of Brox et al.[28] contain large errors in both blurry and clean regions. Although Portz et al.[9] applies the blur-robust flow technique, many errors are still produced. Not only due to its inaccurate linear motion approximation, but also due to its deblurring approach. Without the directional filter processing and the segmented local deblurring operation, its motion blur violates some useful information. The method of MDP[25] preforms much better than methods Portz et al.[9] and Brox et al.,[28] but fails at blurred regions. Like the *sign* sequence [Fig. 8(c)], due to

Table 3 Performance on the typical spatially varying motion blur testing sequences from Wul and Black.[32] For the *elephant* sequence, AEE measures the errors of frame 3 and frame 4. For the *desert* sequence, AEE measures the errors of frame 5 and frame 6. Ave.AEE measures the average error of all the frames. SAEE and Ave. SAEE measure the sampled error and the sampled average error, respectively.

	Elephant				Desert			
Method	AEE	SAEE	Ave. AEE	Ave. SAEE	AEE	SAEE	Ave. AEE	Ave. SAEE
Brox et al.[28]	5.324	4.331	4.946	3.314	2.139	0.543	2.283	0.752
MDP[25]	4.800	4.190	4.127	3.205	1.034	0.305	1.208	0.445
Portz et al.[9]	6.287	4.662	5.885	3.866	1.899	0.890	1.950	0.945
Ours	4.747	4.103	4.118	3.146	0.833	0.254	1.033	0.407

Fig. 6 Visual comparison on the real sequence *magazine*. (a) Frame 2. Results of: (b) Brox et al.,[28] (c) Xu et al.,[25] (d) Portz et al.,[9] and (e) ours.

Fig. 7 Visual comparison on the real sequence *hand*. (a) Frame 2. Results of: (b) Brox et al.,[28] (c) Xu et al.,[25] (d) Portz et al.,[9] and (e) ours.

Fig. 8 Visual comparison on the real sequence *sign*. (a) Frame 2. Results of: (b) Brox et al.,[28] (c) Xu et al.,[25] (d) Portz et al.,[9] and (e) ours.

Fig. 9 Visual comparison on the real sequence *bike*. (a) Frame 2. Results of: (b) Brox et al.,[28] (c) Xu et al.,[25] (d) Portz et al.,[9] and (e) ours.

lack of discriminative deblurring, the blurry information in the sky above the sign is mixed with the *sign*. This problem can also be observed in Fig. 9(c), where the *bike* tire is mixed with the rider. In contrast, our method improves these drawbacks [see Figs. 8(e) and 9(e)]. Clean and blurred regions are clearly distinguished, shapes are more precisely recovered, and motion boundaries at both clean and spatially varying motion blur regions are well-preserved.

6 Conclusions

In this paper, we have proposed an effective optical flow method that can handle spatially varying motion blur. We extend the baseline method of Portz et al.[9] in two aspects: the first aspect that we improve is to modify the data term by matching the detected nonuniform motion blur, which is implemented according to three steps. First, we introduce the directional filter to refine the pre-estimated blur kernel to

improve the deblurring performance. Second, we apply the learned blur maps method to segment the image into blur and clean regions, and only deblur the detected blur regions instead of the whole image to reduce deblurring caused errors. Finally, we present a downsample-interpolation technique to improve the blur detection efficiency. Experimental results show that 75% or more computational time can be saved. The second aspect in which improve the blurring is by improving the regularization term by proposing an IEPR technique. This technique reduces edge violations caused by motion blur and preserves motion boundaries. With these improvements, our algorithm produces more accurate results and significantly improves the efficiency compared to common baseline methods. There are several avenues for future work. One important challenge is to improve the blur detection and deblurring efficiency, as it still costs about 50% of the run-time of the whole optimization. Another challenge is to set the weights of the detected blurred boundary pixels more appropriately. The manner employed in this work to simply set them to one leaves room for improvement. Setting these weights automatically based on the input image is the topic of future work.

Acknowledgments

This publication was supported by the China Scholarship Council (CSC).

References

1. Z. Tu et al., "A combined post-filtering method to improve accuracy of variational optical flow estimation," *Pattern Recognit.* **47**(5), 1926–1940 (2014).
2. B. Horn and B. Schunck, "Determining optical flow," *Artif. Intell.* **17**, 185–203 (1981).
3. J. Barron et al., "Performance of optical flow techniques," in *Proc. Computer Vision and Pattern Recognition (CVPR)*, pp. 236–242 (1992).
4. S. Negahdaripour, "Revised definition of optical flow: integration of radiometric and geometric cues for dynamic scene analysis," *IEEE Trans. Pattern Anal. Mach. Intell.* **20**, 961–979 (1998).
5. J. Weber and J. Malik, "Robust computation of optical flow in a multi-scale differential framework," *Int. J. Comput. Vision* **14**, 67–81 (1995).
6. Z. Tu, C. V. Gemeren, and R. C. Veltkamp, "Improved color patch similarity measure based weighted median filter," in *Proc. Asian Conf. Computer Vision (ACCV)*, Vol. **9007**, pp. 413–427 (2015).
7. W. Li et al., "Robust optical flow estimation for continuous blurred scenes using RGB-motion imaging and directional filtering," in *Proc. Winter Applications of Computer Vision (WACV)* (2014).
8. I. M. Rekleitis, "Optical flow recognition from the power spectrum of a single blurred image," in *Proc. Int. Conf. Image Processing (ICIP)*, pp. 791–794 (1996).
9. T. Portz, L. Zhang, and H. Jiang, "Optical flow in the presence of spatially-varying motion blur," in *Proc. Computer Vision and Pattern Recognition (CVPR)*, pp. 1752–1759 (2012).
10. L. Xu and J. Jia, "Two-phase kernel estimation for robust motion deblurring," *Lec. Notes Comput. Sci.* **6311**, 157–170 (2010).
11. A. Goldstein and R. Fattal, "Blur-kernel estimation from spectral irregularities," *Lec. Notes Comput. Sci.* **7576**, 622–635 (2012).
12. Y. Yitzhaky and N. S. Kopeika, "Identification of blur parameters from motion blurred images," *Graphical Models Image Process.* **59**, 310–320 (1997).
13. S. Cho and S. Lee, "Fast motion deblurring," *ACM Trans. Graphics* **28** (2009).
14. H. Sun et al., "Motion blur parameters identification from radon transform image gradients," in *Annual Conf. of IEEE Industrial Electronics*, Vol. 59, pp. 2098–2103 (2009).
15. Y. Tai and S. Lin, "Motion-aware noise filtering for deblurring of noisy and blurry images," in *Proc. Computer Vision and Pattern Recognition (CVPR)*, pp. 17–24 (2012).
16. NeatImage, http://www.neatimage.com/.
17. L. Zhong et al., "Handling noise in single image deblurring using directional filters," in *Proc. Computer Vision and Pattern Recognition (CVPR)*, pp. 612–619 (2013).
18. J. Shi, L. Xu, and J. Jia, "Discriminative blur detection features," in *Proc. Computer Vision and Pattern Recognition (CVPR)*, pp. 2965–2972 (2014).
19. Z. Hu and M. Yang, "Good regions to deblur," *Lec. Notes Comput. Sci.* **7576**, 59–72 (2012).
20. L. Alvarez et al., "A PDE model for computing the optical flow," in *XVI Congreso de Ecuaciones Diferenciales y Aplicaciones*, pp. 1349–1356, Las Palmas de Gran Canaria (1999).
21. L. Alvarez, J. Weickert, and J. Sánchez, "Reliable estimation of dense optical flow fields with large displacements," *Int. J. Comput. Vision* **39**, 41–56 (2000).
22. C. Schnorr, "Segmentation of visual motion by minimizing convex non-quadratic functionals," in *Proc. Int. Conf. on Image Processing (ICIP)*, pp. 661–663 (1994).
23. J. Weickert and C. Schnorr, "A theoretical framework for convex regularizers in PDE–based computation of image motion," *Int. J. Comput. Vision* **45**, 245–264 (2001).
24. A. Wedel et al., "Structure- and motion-adaptive regularization for high accuracy optic flow," in *Proc. Int. Conf. Computer Vision (ICCV)*, pp. 1663–1668 (2009).
25. L. Xu, J. Jia, and Y. Matsushita, "Motion detail preserving optical flow estimation," *IEEE Trans. Pattern Anal. Mach. Intell.* **34**, 1744–1757 (2012).
26. D. Sun, S. Roth, and M. J. Black, "Secrets of optical flow estimation and their principles," in *Proc. Computer Vision and Pattern Recognition (CVPR)*, pp. 2432–2439 (2010).
27. Z. Tu et al., "Weighted root mean square approach to select the optimal smoothness parameter of the variational optical flow algorithms," *Opt. Eng.* **51**, 037202 (2012).
28. T. Brox, A. Bruhn, and N. Papenberg, "High accuracy optical flow estimation based on a theory for warping," *Lec. Notes Comput. Sci.* **3024**, 25–36 (2004).
29. A. Wedel et al., "An improved algorithm for TV–L1 optical flow," *Lec. Notes Comput. Sci.* **5064**, 23–45 (2008).
30. S. Baker et al., "A database and evaluation methodology for optical flow," *Int. J. Comput. Vision* **92**, 1–31 (2011).
31. D. J. Butler et al., "A naturalistic open source movie for optical flow evaluation," *Lec. Notes Comput. Sci.* **7577**, 611–625 (2012).
32. J. Wul and M. J. Black, "Modeling blurred video with layers," *Lec. Notes Comput. Sci.* **8694**, 236–252 (2014).

Zhigang Tu received his MPhil PhD in image processing in the School of Electronic Information, Wuhan University, China, 2008. Since September 2011, he has been with the Multimedia and Geometry Group at Utrecht University, Netherlands. His current research interests include optical flow estimation, super-resolution construction, multimedia systems and technologies, human–computer interaction.

Ronald Poppe received his PhD in computer science from the University of Twente, the Netherlands. In 2009, 2010, and 2012, he was a visiting researcher at Delft University of Technology, Stanford University, and University of Lancaster, respectively. Currently, he is an assistant professor at the Information and Computing Sciences Department of Utrecht University. His research interests include the analysis of human behavior from videos and other sensors, the understanding and modeling of humans.

Remco Veltkamp is full professor of multimedia at Utrecht University, Netherlands. His research interests include the analysis, recognition, and retrieval of, and interaction with music, images, and three-dimensional objects and scenes, in particular the algorithmic and experimentation aspects. He has written over 150 refereed papers in reviewed journals and conferences, and supervised 15 PhD theses. He was director of the national project GATE–Game Research for Training and Entertainment.